Evaluation of Novel Designs to Address the Shoulder-belt Entrapment for THOR-50M ATD

Z. Jerry Wang, Stephen Fu, Joseph McInnis, John Arthur

Abstract It was observed in THOR 50M vehicle testing that the shoulder belt moved in medial direction toward the neck, slipped over the shoulder pad collar and became entrapped in the gap adjacent to the lower neck load cell. The entrapment caused the unhuman-like response of the THOR 50M, i.e. higher lateral shear load at the lower neck, lower fore-aft load at the left clavicle, and also reduced the chest deflection in upper left and lower right quadrants. The goal of this research is to address the belt entrapment issue without altering the other responses of the dummy. Three design options were analysed with THOR 50M finite element model. The belt at no-slip condition between the original design and the design change options were analysed to compare the output from the dummy sensors. One of the design options demonstrated the belt entrapment issue was addressed when belt slippage occurred. In the meantime, the dummy response of this design remains unchanged when the belt slippage did not occur. The analysis also showed how the other design options would create unfavourable changes to the other responses of the dummy. A prototype part was made for validation testing in vehicle and sled environments, and the results confirmed the observation from the finite element model analysis.

Keywords Anthropomorphic Test Device, Entrapment, Shoulder Belt, Slippage, THOR.

I. INTRODUCTION

The shoulder-belt entrapment to the neck was reported by Tylko *et al*. [1] in car-to-moving car frontal 40% offset crash test. The belt entrapment occurred in 33 of the 45 tests, or 73% occurrence. In rigid barrier tests, belt entrapment occurred in two out of 13 tests, or 16% occurrence. In a sled test, belt entrapment occurred in two out of the three tests. In general, oblique loading resulting outboard motion increased the belt entrapment occurrence rate. Belt entrapment was associated with greater peak fore-aft and lateral shear at the lower neck, reduced fore-aft loads at the inboard and outboard left clavicle, and reduced fore-aft chest deflections in the upper left and lower right quadrants.

The belt entrapment caused an unusual loading path for the lower neck load cell due to the direct contact between the belt and the load cell or adjacent parts attached to the load cell. One of the major causes was that the strength of the dummy shoulder pad collar was not adequate to retain the belt and prevent it from becoming entrapped. The aim of this study was to compare the ATD outputs of three new should pad designs with the baseline and to select a design that would prevent the shoulder-belt entrapment without changing the other responses of the dummy.

II. METHODS

LS-DYNA 971 was used for the finite element (FE) analysis. Humanetics THOR-50M v1.6 FE model was used as the base model. The shoulder pad design and the friction coefficient between the shoulder belt and the jacket were investigated in the study. Both peak values and CORA [2] analysis were used to objectively evaluate the performance of the shoulder pads.

Z. J. Wang is the chief engineer (e-mail jwang@humaenticsatd.com; tel: +1 248 778 2133), S. Fu is a CAE engineer, J. McInnis is a senior CAD designer and J. Arthur is a senior process engineer, all at Humanetics Innovative Solutions, Inc.

Sled Setup

The simulation sled setup model came from a previous Humanetics project. The overall setup is shown in Fig. 1. The test setup has an oblique angle of 18 degrees, to simulate an oblique loading condition in a vehicle. The occupant was restrained with a generic lap/shoulder belt, but no pretension was applied in the analysis. The feet were rested on a rigid seat pan simulator. The dummy was seated to represent a rear-seat passenger with arms down. Rigid seat pan and seat back were used. The seatback angle was set at 10 degrees from vertical and the seat pan angle was set at 10 degrees from horizontal.

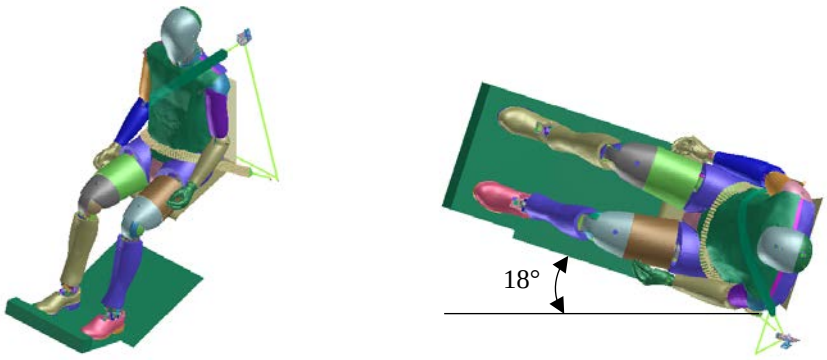

(a) Isometric view (b) Top view

Fig. 1. Sled test setup with 18 degrees oblique angle: (a) isometric view, (b) top view.

The sled deceleration pulse is shown in Fig. 2. The pulse was similar to that used by Tylko *et al*. [1].

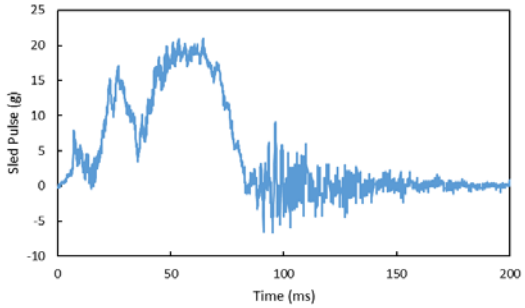

Fig. 2. Sled pulse for the simulation analysis.

Approach Method

To create the no-slip and slip scenarios in the simulations, the friction coefficient between the shoulder belt and the ATD jacket was adjusted. The research was limited to the available validated FE model. The sled test setup, shown in Fig. 1, has rigid surfaces and represent the rear seat configuration, while tests in [1] were vehicle-to-vehicle tests with production seats. However, the simplified sled setup replicated the belt slippage, no belt slippage and belt entrapment scenarios. In addition, the responses of the dummy in this analysis have comparable signal magnitudes between data from this research and the test data in [1].

An alternative collar design, using a rigid plastic material (baseline with hard plastics), was fabricated as a possible solution to the entrapment issue, see Fig. 1(a). A novel concept was to have the part made of two materials: the medial portion near the collar was made of a higher stiffness plastic while the lateral portion material remained unchanged. Two representative design proposals were put forward for this analysis. Design “straight split" has a simple, straight split line between the two materials with different stiffness, see Fig. 1(b). After the analysis of “straight split” design, it was found that the straight split, which offered simplicity in terms of manufacturing, was not sufficient to maintain the other responses of the dummy. A few different split profiles were evaluated in terms of both manufacturability and ATD performance. A final design, referred to as design “profiled split” in this paper, shown in Fig. 3(c) with a complex split profile, was identified as the best among the solutions.

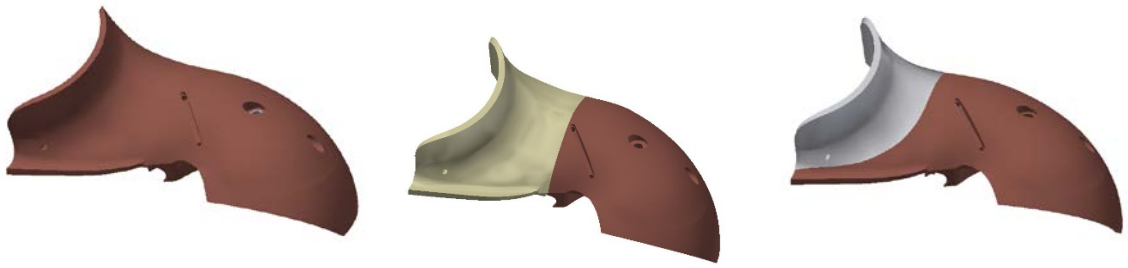

(a) (b) (c)

Fig. 3. Design Proposals: (a) baseline, (b) straight split, (c) profiled split (patent pending).

Simulation Matrix

Four shoulder designs were evaluated in this study. The baseline represents the standard THOR-50M shoulder pad design. The baseline design with hard plastics material, straight split and profiled split designs are alternative design options presented in this paper to illustrate the criteria used for design selection. The simulation matrix is summarized in Table I.

TABLE I
CASE STUDY MATRIX

Case #	Shoulder Pad Designs	Friction Coefficient Between Belt and ATD Jacket
1	Baseline, Fig. 1(a)	0.3
2	Baseline, Fig. 1(a)	0.1
3	Baseline with hard plastics, Fig. 1(a)	0.3
4	Baseline with hard plastics, Fig. 1(a)	0.1
5	Straight Split, Fig. 1(b)	0.3
6	Straight Split, Fig. 1(b)	0.1
7	Profiled Split, Fig. 1(c)	0.3
8	Profiled Split, Fig. 1(c)	0.1

III. RESULTS

From the preliminary testing and simulation, it was obvious that a stiffer shoulder pad collar was capable of preventing belt entrapment. Based on this observation, the investigation was narrowed down to compare the ATD-measured responses from the new designs with the baseline. Under a no-slip condition, i.e. the belt won't be entrapped during the test, the desired new design was expected to match the baseline responses. Under a slip condition, i.e. the belt would slip in the test, the new design was expected to prevent belt entrapment.

It was observed that the shoulder belt would not slip when the friction coefficient was set at the value of 0.3 for the test setup, as described previously, and that the shoulder belt would always slip when the friction coefficient was set at 0.1. Therefore, these two values were chosen for the analysis.

For the no slip condition with friction coefficient 0.3, the lower neck force x and y, left clavicle forces and thoracic displacements were compared. The head acceleration and left femur load, where difference was observed in Tylko *et al.* [1], were not analysed in this study since there was no airbag or other vehicle interior representation in the analysis for meaningful comparison. The data with 0.3 friction coefficient was plotted in the appendix.

The peak values for the analysis are summarised in Table II and also shown in Fig. 1 and Fig. 2. Overall, the "profiled split" design had the closest peak values compared to the baseline design, as shown in Fig. 1. The "straight split" is the second best option and the baseline with hard plastic material is the third best. No significant difference was observed in the thoracic displacements among all four cases (Fig. 2).

TABLE II
PEAK VALUES OF THE MONITORED CHANNELS

	Baseline	Baseline with Stiffer Material	Straight Split	Profiled Split
Lower Neck Fx (kN)	-1.49	-2.12	-1.76	-1.86
Lower Neck Fy (kN)	-0.49	-0.54	-0.57	-0.61
Left Clavicle Medial Fx (kN)	-0.76	-0.82	-0.74	-0.77
Left Clavicle Medial Fz (kN)	0.49	0.41	0.32	0.40
Left Clavicle Lateral Fx (kN)	-0.85	-1.94	-1.25	-0.90
Left Clavicle Lateral Fz (kN)	0.70	0.84	0.49	0.84
Right Clavicle Medial Fx (kN)	0.91	1.01	1.05	0.85
Thoracic IR-TRACC DX – UL (mm)	-35.1	-34.1	-34.9	-36.1
Thoracic IR-TRACC DX – UR (mm)	-65.2	-64.5	-64.1	-65.0
Thoracic IR-TRACC DX – LL (mm)	-15.5	-14.7	-16.4	-16.5
Thoracic IR-TRACC DX – LR (mm)	-54.5	-54.5	-54.6	-54.6

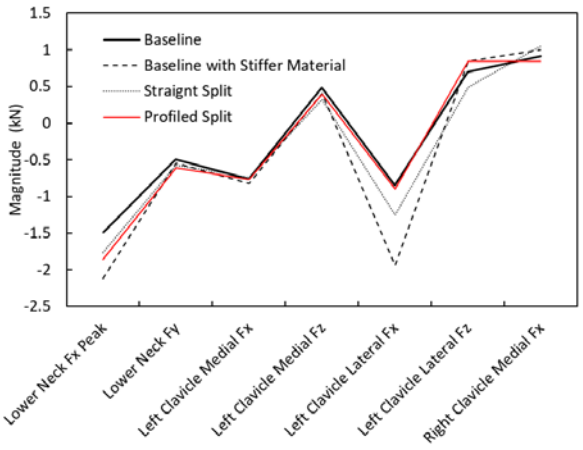

Fig. 1. Lower neck and clavicle load cell output of the four cases analysed.

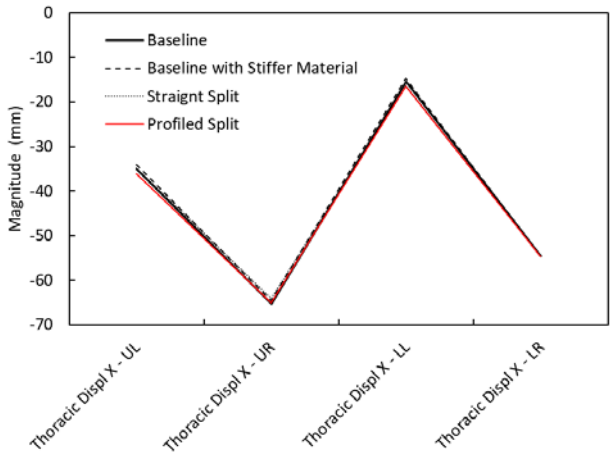

Fig. 2. Thoracic displacements comparison in four IR-TRACC locations of the four cases.

CORA analysis was conducted to objectively quantify the responses of the new designs against the baseline. CORA scores for all monitored channels per the design proposal are shown in Table III. The "profiled split" design has the highest average CORA score of 0.7851. The baseline with stiffer material has an overall average CORA score of 0.7472, while the average CORA score for the "straight split" design is 0.6703. The CORA scores for baseline with stiffer material and the "straight split" design indicated contrary results than the peak values presented above. However, both methods indicate that the "profiled split" would be the preferred solution.

TABLE III
CORA SCORES OF THE MONITORED CHANNELS FOR EACH DESIGN PROPOSAL

Data Channels	Baseline with Stiffer Material	Straight Split	Profiled Split
Lower Neck Fx	0.7602	0.7992	0.8292
Lower Neck Fy	0.8378	0.6598	0.7359
Left Clavicle Medial Fx	0.6069	0.6015	0.6370
Left Clavicle Medial Fz	0.6408	0.4138	0.7488
Left Clavicle Lateral Fx	0.7057	0.6203	0.8010
Left Clavicle Lateral Fz	0.6419	0.4940	0.7044
RIGHT Clavicle Medial Fx	0.7716	0.7773	0.8612

RIGHT Clavicle Medial Fz	0.5015	0.2131	0.3405
RIGHT Clavicle Lateral Fx	0.5387	0.4288	0.6323
RIGHT Clavicle Lateral Fz	0.4791	0.4261	0.7574
THORAX IR-TRACC Dx UL	0.9933	0.9970	0.9900
THORAX IR-TRACC Dx UR	0.9953	0.9940	0.9996
THORAX IR-TRACC Dx LL	0.9922	0.9590	0.9559
THORAX IR-TRACC Dx LR	0.9957	0.9997	0.9982
Average	0.7472	0.6703	0.7851

IV. DISCUSSION

The design aim was to maintain the dummy responses as much as possible and also to address the belt entrapment issue. The simulation showed that all three new designs addressed the belt entrapment issue. The focus of the research was to identify which design option had the least influence on the dummy responses. The peak values of the selected channels show that the “profiled split” has the closest response to the base design when comparing the peak values of lower neck load cell, clavicle load and thoracic displacements. The CORA analysis, which compares the time history of each channel, showed that the “profiled split” design provided the highest correlation to the baseline response, which is consistent with the results achieved by comparing the peak values.

On the right clavicle medial load Fz, it was noticed the CORA scores are low for all three designs and the “profiled split” has the lowest score of 0.3405. Since the shoulder belt did not directly interact with the right clavicle load cell in the case analyzed in this paper, the load was relatively low and well below the injurious load level, therefore not a critical data channel to considered in the rating.

Based on these findings, the “profiled split” design is recommended as the best replacement of the baseline design that addressed the belt entrapment problem in the FE analysis.

It was concerned that the baseline design with hard plastic may create unhuman like range of motion. However, the shoulder trajectories did not show any significant differences among the cases analyzed in this paper.

Vehicle tests results obtained by Transport Canada confirmed that the belt entrapment was eliminated by the “profiled split” design. While under the condition with no-slippage condition, the dummy response with “profiled split” shoulder pad are comparable to the results of the “baseline” design from preliminary analysis. The results will be published in the future for further confirmation.

V. CONCLUSIONS

Three difference shoulder designs that could address the belt entrapment issue were analysed in an oblique sled test condition. All three designs proved capable of preventing belt entrapment. Comparing the data in peak values and time history (CORA analysis), the “profiled split” design had most similar dummy response compared to the “baseline” design and is therefore recommended to replace the standard shoulder pad as the best solution to resolve the problem of belt entrapment. Vehicle testing was planned to further confirm the results in this paper.

VI. LIMITATIONS

The cased analyzed in this study is very limited and may not represent any real world vehicle crash test exactly. The sled configuration represents a rear seat configuration, which differs the entrapment issue identified in front seat configuration. By no means the analysis in this paper can represent the small vehicle-to-vehicle small overlap test where the problem was identified, but a simplified setup to optimize the shoulder pad design for further validation in vehicle testing.

VII. ACKNOWLEDGEMENT

The authors would like to thank Ms. Suzanne Tylko of Transport Canada, Ms. Kathy Tang and the PMG team for providing videos and detailed information to elucidate the details of the problem. In addition, Transport Canada kindly offered to test the prototype part to validate the new design.

VIII. REFERENCES

[1] Tylko, S., Tang, K., Giguère, F., Bussières, A. (2018) Effects of shoulder-belt slip on the kinetics and kinematics of the THOR. *Proceedings of IRCOBI Conference*, 2018, Athens, Greece.

[2] Gehre, C., Gades, H., Wernicke, P. (2009) Objective rating of signals using test and simulation responses. *21st ESV Conference Proceedings*, June 13–16 2009, Stuttgart, Germany.

IX. APPENDIX

Data Plots for friction coefficient of 0.3 between the shoulder belt and the ATD jacket.

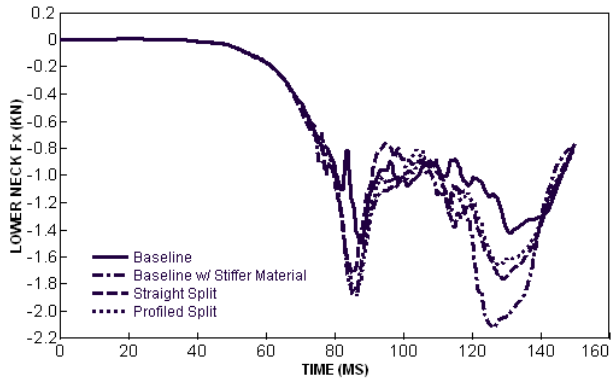

Fig. 3. Lower neck force in x direction.

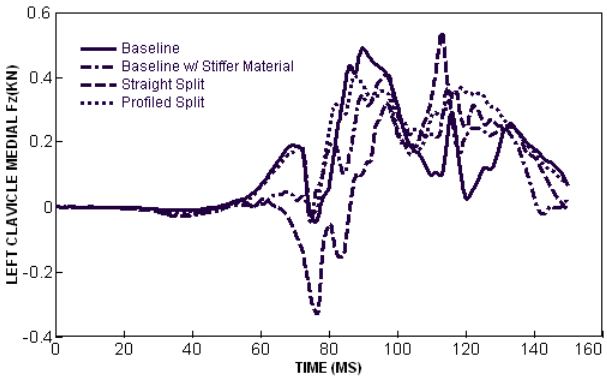

Fig. 6. Left clavicle medial force in z direction.

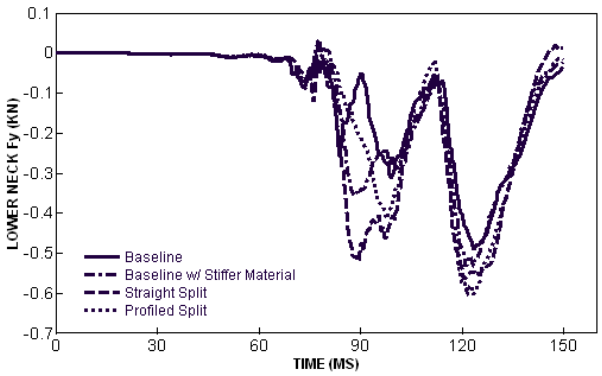

Fig. 4. Lower neck force in y direction.

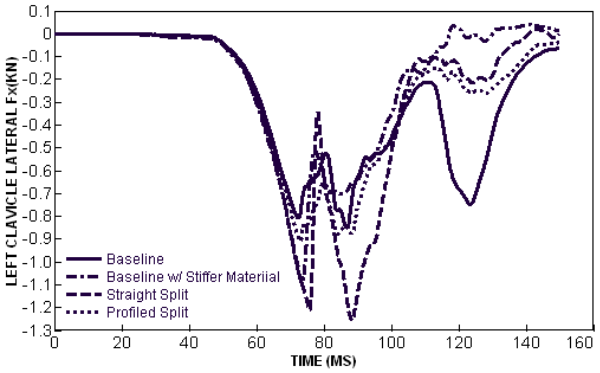

Fig. 7. Left clavicle lateral force in x direction.

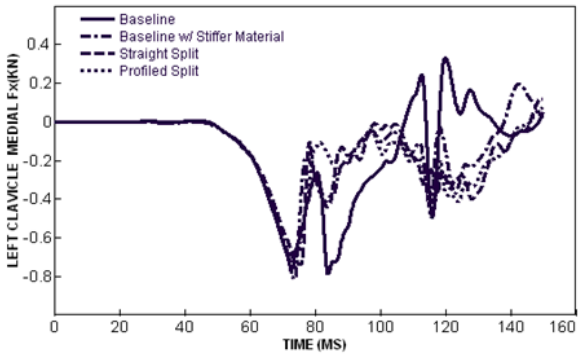

Fig. 5. Left clavicle medical force in x direction.

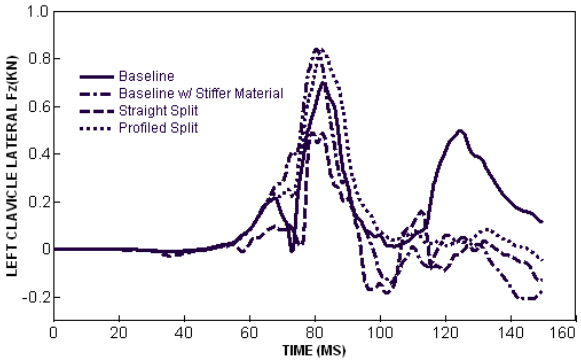

Fig. 8. Left clavicle lateral force in z direction.

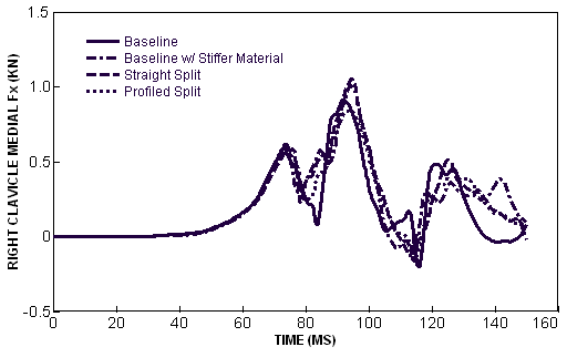

Fig. 9. Right clavicle medial force in x direction.

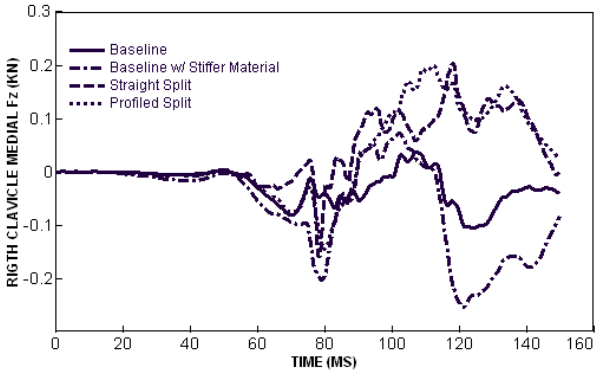

Fig. 10. Right clavicle medial force in z direction.

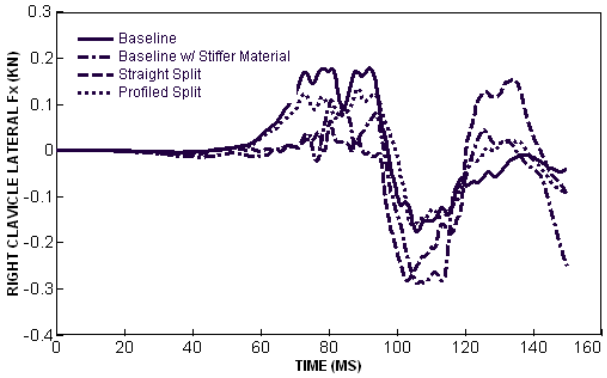

Fig. 11. Right clavicle lateral force in x direction.

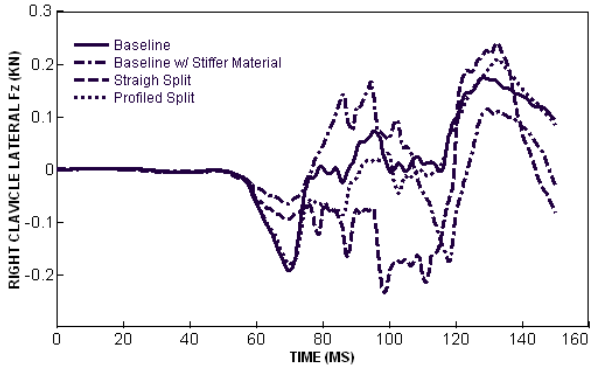

Fig. 12. Right clavicle lateral force in z direction.

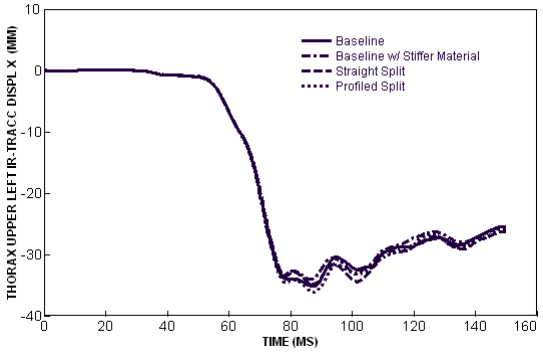

Fig. 13. Thoracic x displacement of the upper left IR-TRACC.

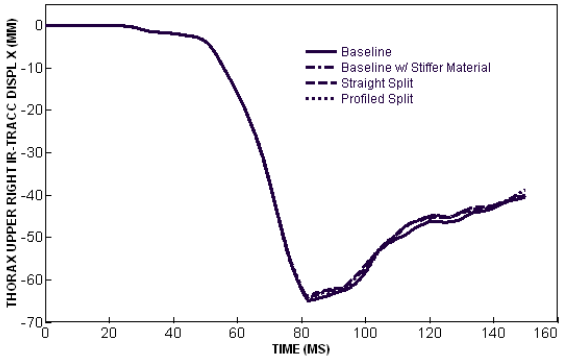

Fig. 14. Thoracic x displacement of the upper right IR-TRACC.

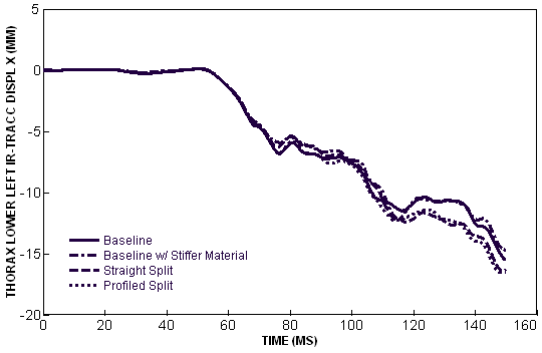

Fig. 15. Thoracic x displacement of lower left IR-TRACC.

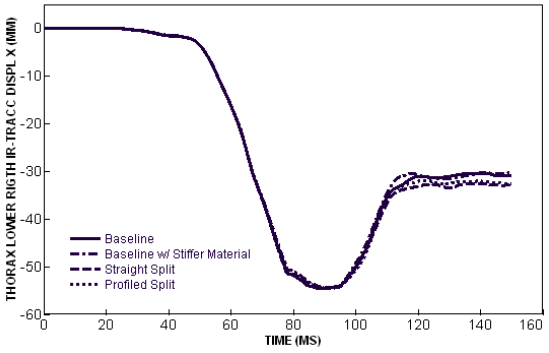

Fig. 16. Thoracic x displacement of lower right IR-TRACC.